

Supernova Remnants in Molecular Clouds

Roger A. Chevalier

*Department of Astronomy, University of Virginia
P.O. Box 3818, Charlottesville, VA 22903*

Abstract. Supernovae are expected to occur near the molecular material in which the massive progenitor star was born, except in cases where the photoionizing radiation and winds from the progenitor star and its neighbors have cleared out a region. The clumpy structure in molecular clouds is crucial for the remnant evolution; the supernova shock front can become radiative in the interclump medium and the radiative shell then collides with molecular clumps. The interaction is relevant to a number of phenomena: the hydrodynamics of a magnetically supported dense shell interacting with molecular clumps; the molecular emission from shock waves, including the production of the OH 1720 MHz maser line; the relativistic particle emission, including radio synchrotron and γ -ray emission, from the dense radiative shell; and the possible gravitational instability of a compressed clump.

INTRODUCTION

Massive stars are born in molecular clouds and those with masses $\gtrsim 8 M_{\odot}$ end their lives as supernovae after $\lesssim 3 \times 10^7$ years. This age is less than the typical age of molecular clouds so that the supernovae may explode in the vicinity of molecular cloud material. Early studies of the interaction assumed that the supernovae interacted directly with molecular cloud material, with density $n_H = 10^4 - 10^5 \text{ cm}^{-3}$ [1], [2]. At these high densities, the supernova remnant evolves on a timescale of 10's of years during which it is a luminous infrared source.

Such sources have not been clearly observed. However, supernova remnant interaction with molecular gas has been observed, starting with the remnant IC 443 [3]. Continued observations have shown IC 443 to be one of the best cases of molecular cloud line emission [4]. The emission appears to be associated with shock interaction with dense clumps, as expected in a molecular cloud; the point of view adopted here involves the expansion of the supernova remnant shell in the interclump medium of a cloud with some collisions with clumps [5].

THE SUPERNOVA SURROUNDINGS

A crucial point for the evolution of supernova remnants in molecular clouds is the clumpy structure of these clouds. The basic picture that has emerged is of dense clumps with most of the mass embedded in a lower density interclump medium. Blitz [6] notes some properties of typical Giant Molecular Clouds: total mass $\sim 10^5 M_\odot$, diameter ~ 45 pc, H_2 density in clumps of 10^3 cm^{-3} , interclump gas density in the range $5\text{--}25$ H atoms cm^{-3} , and clump filling factor of $2\text{--}8\%$. The clumps have an approximate power law mass spectrum, such that there are more small clumps, but most of the mass is in the large clumps. There have been recent attempts to model the clump properties in terms of MHD (magnetohydrodynamic) turbulence [7,8]. In this case, the clumps may be transitory features in the molecular cloud.

If the dense clumps are confined by the interclump pressure, a pressure $p/k \approx 10^5 \text{ K cm}^{-3}$ is needed [6]. Even if the clumps are features in a fluctuating velocity field and are not necessarily confined, a comparable pressure is needed to support the clouds against gravitational collapse. The thermal pressure in the interclump gas is clearly too small and magnetic fields are a plausible pressure source. Studies of the polarization of the light from stars behind molecular clouds implies that the interclump magnetic field does have a uniform component [9]. Setting $B_o^2/8\pi$ equal to the above pressure yields $B_o = 19p_5^{1/2} \mu\text{G}$, where B_o is the uniform field component and p_5 is p/k in units of 10^5 K cm^{-3} . However, a uniform magnetic field would not provide support along the magnetic field and would not explain the large line widths observed in clouds. An analysis of the polarization and Zeeman effect in the dark cloud L204 shows consistency with equal contributions to the pressure from a uniform field and a fluctuating, nonuniform component [9]. The uniform component is then $B_o = 13p_5^{1/2} \mu\text{G}$. The magnetic field strength deduced in L204 is consistent with this value.

The molecular cloud can be influenced by stellar mass loss and photoionization by the progenitor star before the supernova. The effect of these processes can be to remove molecular gas from the vicinity of the central star. Draine and Woods [10] found that stars with initial mass $\lesssim 20 M_\odot$ in clouds of density $n_H \gtrsim 10^2 \text{ cm}^{-3}$ would have such a small effect that the surroundings could be treated as homogeneous in discussing the blast wave evolution. For a $25 M_\odot$ star, they found the presupernova effects to be small provided $n_H \gtrsim 10^3 \text{ cm}^{-3}$. In an interclump medium with $n_H \approx 10 \text{ cm}^{-3}$, Chevalier [5] found that stars with mass $\lesssim 12 M_\odot$ would clear a region with radius $\lesssim 5$ pc around the star because of the effects of photoionization and winds. The high pressure of the molecular cloud plays a role in limiting the effects of the progenitor star. If the massive star has a significant velocity ($\sim 5 \text{ km s}^{-1}$), the star can move into a region of undisturbed cloud material and the progenitor star effects are lessened [10]. On the other hand, massive stars tend to form in clusters and the immediate environment of a star could be affected by nearby, more massive stars. In a sparse cluster, it is still possible for a massive star to interact with its

natal cloud material.

THE CASE OF IC 443

The remnant IC 443 shows many of the features that characterize molecular cloud interaction. The remnant appears to be interacting with a relatively low mass molecular cloud ($\lesssim 10^4 M_\odot$) that is primarily in front of the remnant [11]. This low mass suggests that there were few or no massive stars which would be likely to disrupt the cloud with their photoionizing fluxes and winds. A lower mass Type II supernova could thus interact directly with the molecular cloud. I take the distance to the remnant to be 1.5 kpc [12].

The morphology of the remnant is a shell in the molecular cloud region, with an apparent “break-out” region to the southwest (see [13] for an X-ray image and [14] for a radio image). I consider the shell part of the remnant to be interacting with the molecular cloud. Fesen and Kirshner [12] found that the spectra of the optical filaments in this region imply an electron density for the [S II] emitting region of $\lesssim 100$ to 500 cm^{-3} and shock velocities in the range $65 - 100 \text{ km s}^{-1}$. If the magnetic field does not limit the compression at a temperature $\sim 10^4 \text{ K}$, the preshock density implied by the higher density filaments is $10 - 20 \text{ cm}^{-3}$. The filaments with a lower density may have their compression limited by the magnetic field. These observations point to a radiative phase of evolution for the remnant in the interclump medium of the molecular cloud. The cooling shock front is expected to build up a shell of HI [15]. For an ambient density of 15 cm^{-3} and a radius of 7.4 pc, the total swept-up mass is $1000 M_\odot$ for a half-sphere. HI observations suggest that there is $\sim 1000 M_\odot$ of shocked HI in the northeast shell part of the remnant, with velocities up to $\sim 110 \text{ km s}^{-1}$ [16]. These results are in quantitative accord with expectations for a 10^{51} erg supernova in a medium with $n_o = 15 \text{ cm}^{-3}$ [5,15], if account is taken of the fact that some energy has been released in the blow-out region.

In a restricted region across the central, eastern part of IC 443, a rich spectrum of molecular emission has been observed [4,17]. A set of spectroscopically distinct CO clumps has been labelled A–G [3,18], although the H_2 emission indicates that the clumps are associated through a filamentary molecular structure [19]. These clumps, with sizes $\sim 1 \text{ pc}$, have masses of $3.9 - 41.6 M_\odot$ as deduced from ^{12}CO lines [20]. The corresponding densities, $n_H \lesssim 500 \text{ cm}^{-3}$, are low but should be regarded as lower limits because the ^{12}CO emission is assumed to be optically thin. Also, there is likely to be density structure within individual clumps. Analysis of absorption in one place yielded a preshock density of $n(\text{H}_2) \approx 3,000 \text{ cm}^{-3}$ [4]. The properties of these clumps are consistent with those seen in quiescent molecular clouds. High spatial resolution is possible in the H_2 infrared lines, which show clumps down to a scale of $1''$ ($2 \times 10^{16} \text{ cm} = 0.007 \text{ pc}$ at a distance of 1.5 kpc) but not smaller [17]. The emission has a knotty appearance that is unlike the filamentary appearance of the optical emission in IC 443 and the H_2 emission in the Cygnus Loop [17].

This type of structure is consistent with the possible fractal structure of molecular clumps [8].

The 2MASS survey has provided a K_s band image of IC 443 that is likely to be dominated by shocked H_2 emission [21]. The image clearly shows a ridge of emission passing from the south to the central part of the remnant. The J and H band images with the 2MASS survey show emission from the northeast part of the remnant, which is likely to be $[\text{Fe II}]$ emission from the $\sim 100 \text{ km s}^{-1}$ shock wave. Observations of the $[\text{O I}] 63 \mu\text{m}$ line with *ISO* (Infrared Space Observatory) show that it is particularly strong in the northeast shell region [21], which implies that it is also from the $\sim 100 \text{ km s}^{-1}$ shock. This is consistent with expectations that most of the $[\text{O I}] 63 \mu\text{m}$ line luminosity should be from the shock front in the interclump medium [5].

The interpretation of the molecular line strengths is still controversial, but the emission is most consistent with that from a partially dissociating J (jump)-type shock [4,17,19,22]. The required shock velocity, $25 - 30 \text{ km s}^{-1}$, is consistent with the velocities observed in the strongest emission. The dissociated H_2 can be observed as a high column density of shocked HI at the positions of the clumps [23]. Following [5], I interpret the clump shock as being driven by the radiative shell in the interclump region (Fig. 1); this can generate a pressure in the interaction region

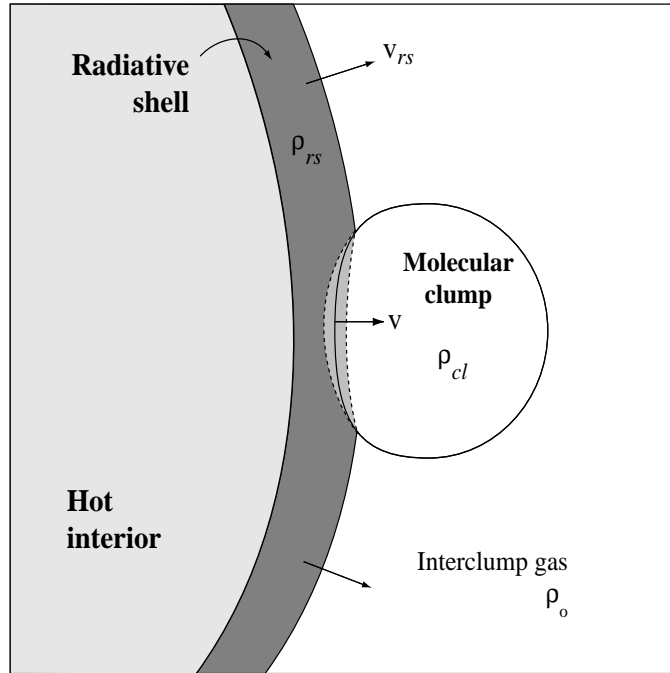


FIGURE 1. Interaction of a radiative shell, moving at velocity v_{rs} , with a molecular clump. The interaction generates a dense slab bounded by shock waves (dashed lines) and moving at velocity v . The densities of the molecular clump, ρ_{cl} , the radiative shell, ρ_{rs} , and the interclump medium, ρ_o , are indicated. From [5].

significantly above that expected for ram pressure equilibrium. For a clump shock velocity $v = 25 - 30 \text{ km s}^{-1}$ and a radiative shell velocity $v_{rs} = 100 \text{ km s}^{-1}$, the ratio of clump density to shell density ρ_{cl}/ρ_{rs} is in the range $5.4 - 9.0$. The density ratio can vary significantly with relatively little effect on the shock velocity. The clump shock velocity is consistent with shell density $n_{rs} = 500 \text{ cm}^{-3}$ and preshock clump density $n_{cl} = 3000 \text{ cm}^{-3}$, which are plausible values. The ratio of postshock pressure in the clump to that in the interclump medium (with $n_o = 15 \text{ cm}^{-3}$) is 18.

The column density through the radiative shell is $N_H \approx n_o R/3 \approx 10^{20} \text{ cm}^{-2}$. For $n_{cl} = 3000 \text{ cm}^{-3}$, the column density through the clumps is $10^{22} \ell_{pc} \text{ cm}^{-2}$, where ℓ_{pc} is the path length through the clump in pc. The larger observed clumps are thus expected to be passed over by the radiative shell and left in the interior of the remnant. For clumps with a size $\lesssim 0.02 \text{ pc}$, the shock front breaks out of the clump first and there is the possibility of further acceleration by the radiative shell. The initial shock front through the clump may not dissociate molecules, which are then accelerated by the shell. Low column densities of high velocity molecular gas can be produced in this way. High velocity molecular gas has been observed in IC 443 at the edge of one of the clumps [24].

Cesarsky et al. [25] have observed H_2 rotational lines from clump G with *ISO*. They find that the line fluxes are consistent with a shock velocity $\sim 30 \text{ km s}^{-1}$, a preshock density $\sim 10^4 \text{ cm}^{-3}$, and an evolutionary time of $1,000 - 2,000$ years. At constant velocity, the shock has penetrated $\sim 0.03 - 0.06 \text{ pc}$ into the clump. This result is consistent with the clump interaction scenario.

Another important diagnostic of the molecular interaction is the OH 1720 MHz maser line, which Claussen et al. [14] find to be associated with clump G in IC 443. Lockett et al. [26] examined the pumping of the maser and found that the emission implies temperatures of $50 - 125 \text{ K}$ and densities $\sim 10^5 \text{ cm}^{-3}$; the shock must be *C*-type. An important aspect of the OH maser observations is that it is possible to estimate the line-of-sight magnetic field from the Zeeman effect. Although they do not have a result for IC 443, Claussen et al. [14] find $B_{||} \approx 0.2 \text{ mG}$ for the maser spots in W28 and W44. This field strength is compatible with the field strength expected in the radiative shells of the supernova remnants [5].

In addition to the molecular line emission, IC 443 is a source of nonthermal continuum emission. At low frequencies, the power law radio spectrum is likely to be explained by synchrotron emission. The observed spectral index, $F_\nu \propto \nu^{-0.36}$ [27], implies a particle energy spectrum of the form $N(E) \propto E^{-1.72}$. Duin and van der Laan [28] explained the radio emission by the shock compression of the ambient magnetic field and relativistic electrons. First order Fermi acceleration should be included and is consistent with the observations if ambient cosmic rays are accelerated [5,29]. In the shock acceleration of ambient particles, the particle spectrum is maintained in the postshock region if the particle spectrum is flatter than $N(E) \propto E^{-2}$. Chevalier [5] argued that the relatively flat spectrum may be consistent with the Galactic cosmic ray electron spectrum, which is observed to be flat at low energies, perhaps because of Coulomb losses in the interstellar medium.

If particles are injected into first order shock acceleration at a low energy, the

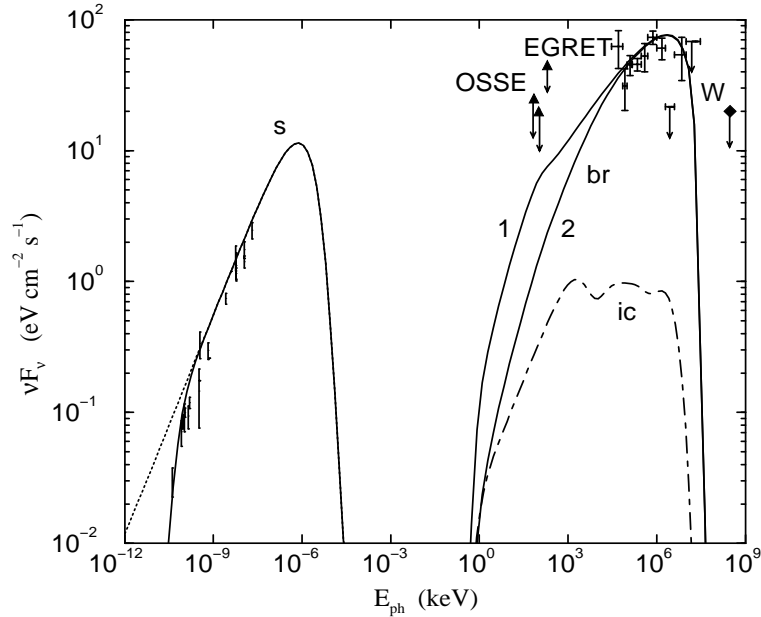


FIGURE 2. Broadband νF_ν spectrum of the shell of IC 443 calculated from a model of nonthermal electron production by a radiative shock with direct injection of electrons from the thermal pool. The shock velocity is 150 km s^{-1} , the interclump number density is 25 cm^{-3} , and the interclump magnetic field is $1.1 \times 10^{-5} \text{ G}$. The two solid curves labeled by numbers 1 and 2 correspond to two limiting values of an MHD turbulence parameter. The extended inverse Compton emission from the whole remnant is shown as a dashed line (ic). The observational data points are from [32] for the *EGRET* source 2EG J0618 +2234 and [27] for the IC 443 radio spectrum. Upper limits for MeV emission are from *OSSE* observations [34]. Upper limits for γ -rays $\geq 300 \text{ GeV}$ are from *Whipple* observations of IC 443 [36]. From [31].

spectrum tends to $N(E) \propto E^{-2}$ in the postshock region in the test particle limit. However, Ostrowski [30] found that second order Fermi acceleration in the turbulent medium near the shock could give rise to a relatively flat spectrum, as observed in IC 443. In another calculation including shock acceleration of electrons from a thermal pool, Bykov et al. [31] found that the combination of nonlinear effects on the shock compression and free-free absorption of the radiation could give rise to the observed spectrum (Fig. 2).

An additional constraint on nonthermal particles comes from the γ -ray detection of IC 443 by the *EGRET* experiment on *CGRO* (Compton Gamma-Ray Observatory) [32], although the poor spatial resolution of the *CGRO* still leaves some doubt about the detection. Assuming that the detection is correct, the emission mechanisms that might contribute to the radiation are electron bremsstrahlung, pion decays, and inverse Compton radiation [33]. A number of studies have fit the γ -ray spectrum of IC 443 with these processes [34,35], but they have assumed

adiabatic shock wave dynamics. In view of the strong evidence for radiative shocks in IC 443, Bykov et al. [31] studied electron injection and acceleration in the context of radiative shock waves in a relatively dense medium. A model with injection of electrons from the thermal pool could approximately fit the observations, with bremsstrahlung being the dominant radiation mechanism (see Fig. 2). As can be seen in Fig. 2, the upper limit on TeV γ -rays from the Whipple Observatory [36] places an important constraint on the high energy part of the particle spectrum.

The continuum radio image of IC 443 [14] shows that although there is some correlation with the molecular emission [21], the shocked molecular clumps do not stand out as sources of radio synchrotron emission. In hard X-ray observations with *ASCA*, Keohane et al. [37] found two emission regions in IC 443, which have also been found in *BeppoSAX* observations [38]. Recent observations with *Chandra* show that the brighter source is likely to be a pulsar wind nebula [39], as indicated by earlier observations [5]. The other source may be associated with the molecular interaction along the southeast rim of the remnant. Keohane et al. [37] suggested that the emission could be synchrotron emission from shock accelerated electrons, but the slow shock velocity in the radiative shock model makes such an interpretation unlikely [5]. Bykov et al. [31] suggested that the emission could be bremsstrahlung from electrons accelerated in ionizing shock waves in relatively dense gas. The evidence for *C*-shocks giving rise to OH maser emission implies non-ionizing shock waves, but different conditions could prevail in different clumps. The prediction is that the shock waves in the interclump gas can produce bremsstrahlung γ -ray emission, while the shock waves in the clump gas can in some cases produce hard X-ray emission.

The radio emission from IC 443 is relatively highly polarized for a supernova remnant, indicating a preferred direction for the magnetic field in the shell [40]. The field direction agrees with that in the ambient cloud, as determined by the polarization of starlight. This is consistent with an ordered magnetic field in the cloud, as mentioned for molecular cloud support in the previous section.

The ordered field observed in radio emission refers to the field in the swept up radiative shell. However, there may also be a uniform component to the magnetic field in the hot interior of the radiative remnant, which would allow heat conduction to operate in the interior. IC 443 is observed to have a relatively isothermal interior with $T \approx 10^7$ K [41]. An isothermal interior with enhanced central X-ray emission is a characteristic of a number of remnants that are interacting with molecular gas. Shelton et al. [42] have discussed a conduction model for the remnant W44, which is a member of this class. They find that the model X-ray emission distribution profile is close to that observed, although it is not as centrally concentrated.

DISCUSSION AND FUTURE PROSPECTS

After a period of neglect, the study of supernova remnants interacting with molecular material has entered a phase of more intense study. In addition to IC 443,

a number of remnants have come in for study. One reason for the increase is the re-discovery of the OH 1720 MHz maser line emission as a signpost of molecular clump interaction. Although initial observations were made more than 30 years ago [43], it was not until after the recent observations by Frail et al. [44] that the importance of the emission for remnant studies was realized. Surveys of remnants [45,46] have yielded 17 remnants with the OH maser line emission out of 160 observed. In addition, Koralesky et al. [47] made VLA observations searching for maser emission toward 20 remnants and found shock excited emission in 3 of them. When remnants with OH maser emission are observed in the CO line, molecular clumps have been observed in a number of cases. Frail and Mitchell [48] found CO clumps associated with the OH emission in W28, W44, 3C 391 and Reynoso and Mangum [49] found such clumps in three other remnants.

Another source of progress has been the availability of infrared observations, especially recently with *ISO*. *ISO* has been instrumental in detecting atomic fine structure lines, molecular lines, and dust continuum emission from remnants that appear to be interacting with molecular gas [50–52]. Of particular interest is the study by Reach and Rho [52] of emission from W28, W44, and 3C 391. They found evidence for interaction with a clumpy medium in which higher pressures were attained at higher densities, as discussed for IC 443. This situation can be explained by a dense radiative shell interacting with molecular clumps. More recently, the 2MASS survey has provided near-infrared imaging of the sky. The 2MASS K_s band image of IC 443 is likely to be dominated by shocked H_2 emission [21]. The detection of supernova remnants in this band thus provides a good indication that molecular interaction is taking place. The advent of the future NASA infrared observatories *SOFIA* and *SIRTF* will allow more complete studies of the density structure in shocked molecular clouds.

Reach and Rho [53] suggest that the mass of compressed gas in the shocked clump in 3C 391 is sufficiently high that self-gravity is significant and that it could eventually form one or more stars. Star formation in shocked supernova clumps cannot be directly verified because the clump collapse time is considerably longer than the age of the supernova remnants. By the time stars have formed, it is difficult to unambiguously discern a supernova trigger. One reason for interest in supernova triggered star formation has been the evidence for extinct radioactivities in the early solar system and this has stimulated computer simulations of the process [54,55]. The observations of supernova remnants in molecular clouds can be useful in providing realistic initial conditions for such simulations.

In cases where massive stars form in a dense cluster, the combined effects of the photoionizing radiation and winds can effectively clear molecular cloud material from the immediate vicinity of the stars. However, observations of the Trapezium cluster in Orion have shown the presence of small, dense gaseous regions, which O’Dell et al. [56] have identified as proplyds (protoplanetary disks). The eventual supernova explosion of one of the massive stars interacts with the disk material; nearby disks are disrupted, but ones farther out can survive [57]. These interactions may have observable consequences in supernova remnants.

The study of supernova remnants in molecular clouds has attracted renewed attention in the past few years and can be expected to blossom with the advent of new observatories and space missions, such as the *ALMA* millimeter array, the *SOFIA* and *SIRTF* infrared observatories, and the *GLAST* γ -ray mission. These observatories will make possible the detailed study of molecular shock waves and γ -ray emission from relativistic particles. The shock waves in molecular clouds provide an important probe of molecular cloud structure, which remains uncertain. A combination of hydrodynamic studies with emission calculations will be useful in elucidating this area.

ACKNOWLEDGMENTS

This work was supported in part by NASA grants NAG5-8232 and NAG5-8088.

REFERENCES

1. Shull, J. M., *ApJ* **237**, 769 (1980)
2. Wheeler, J. C., Mazurek, T. J., and Sivaramakrishnan, A., *ApJ* **237**, 781 (1980)
3. DeNoyer, L., *ApJ* **232**, L165 (1979)
4. van Dishoeck, E. F., Jansen, D. J., and Phillips, T. G., *A&A* **279**, 541 (1993)
5. Chevalier, R. A., *ApJ* **511**, 798 (1999)
6. Blitz, L., in *Protostars and Planets III*, Tucson: Univ. of Arizona, 1993, p. 125
7. Vázquez-Semadeni, E., Ostriker, E. C., Passot, T., and Gammie, C. F., in *Protostars and Planets IV*, Tucson: Univ. of Arizona, 2000, p. 3
8. Williams, J. P., Blitz, L., and McKee, C. F., in *Protostars and Planets IV*, Tucson: Univ. of Arizona, 2000, p. 97
9. Heiles, C., Goodman, A. A. McKee, C. F., and Zweibel, E. G., in *Protostars and Planets III*, Tucson: Univ. of Arizona, 1993, p. 279
10. Draine, B. T., and Woods, D. T., *ApJ* **383**, 621 (1991)
11. Cornett, R. H., Chin, G., and Knapp, G. R., *A&A* **54**, 889 (1977)
12. Fesen, R. A., and Kirshner, R. P., *ApJ* **242**, 1023 (1980)
13. Asaoka, I., and Aschenbach, B., *A&A* **284**, 573 (1994)
14. Claussen, M. J., Frail, D. A., Goss, W. M., and Gaume, R. A., *ApJ* **489**, 143 (1997)
15. Chevalier, R. A., *ApJ* **188**, 501 (1974)
16. Giovanelli, R., and Haynes, M. P., *ApJ* **230**, 404 (1979)
17. Richter, M. J., Graham, J. R., and Wright, G. S., *ApJ* **454**, 277 (1995)
18. Huang, Y.-L., Dickman, R. L., and Snell, R. L., *ApJ* **302**, L63 (1986)
19. Burton, M. G., Hollenbach, D. J., Haas, M. R., and Erickson, E. F., *ApJ* **355**, 197 (1990)
20. Dickman, R. L., Snell, R. L., Ziurys, L. M., and Huang, Y.-L., *ApJ* **400**, 203 (1992)
21. Rho, J., Jarrett, T. H., Cutri, R. M., and Reach, W. T., *ApJ* in press (astro-ph/0010551) (2000)
22. Richter, M. J., Graham, J. R., Wright, G. S., Kelly, D. M., and Lacy, J. H., *ApJ* **449**, L83 (1995)

23. Braun, R., and Strom, R. G., *A&A* **164**, 193 (1986)
24. Tauber, J. A., Snell, R. L., Dickman, R. L., and Ziurys, L. M., *ApJ* **421**, 570 (1994)
25. Cesarsky, D., Cox, P., Pineau des Forets, G., van Dishoeck, E. F., Boulanger, F., and Wright, C. M., *A&A* **348**, 945 (1999)
26. Lockett, P., Gauthier, E., and Elitzur, M., *ApJ* **511**, 235 (1999)
27. Erickson, W. C., and Mahoney, M. J., *ApJ* **290**, 596 (1985)
28. Duin, R. M., and van der Laan, H., *A&A* **40**, 111 (1975)
29. Blandford, R. D., and Cowie, L. L., *ApJ* **260**, 625 (1982)
30. Ostrowski, M., *A&A* **345**, 256 (1999)
31. Bykov, A. M., Chevalier, R. A., Ellison, D. C., and Uvarov, Yu. A., *ApJ* **538**, 203 (2000)
32. Esposito, J. A., Hunter, S. D., Kanbach, G., and Sreekumar, P., *ApJ* **461**, 820 (1996)
33. Gaisser, T. K., Protheroe, R. J., and Stanev, T., *ApJ* **492**, 219 (1998)
34. Sturmer, S. J., Skibo, J. G., Dermer, C. D., and Mattox, J. R., *ApJ* **490**, 619 (1997)
35. Baring, M. G., Ellison, D. C., Reynolds, S. P., Grenier, I. A., and Goret, P., *ApJ* **513**, 311 (1999)
36. Buckley, J. H., et al., *A&A* **329**, 639 (1998)
37. Keohane, J. W., Petre, R., Gotthelf, E. V., Ozaki, M., and Koyama, K., *ApJ* **484**, 350 (1997)
38. Bocchino, F., and Bykov, A. M., *A&A* **362**, L29 (2000)
39. Clearfield, C. R., et al., these proceedings
40. Kundu, M. R., and Velusamy, T., *A&A* **20**, 237 (1972)
41. Petre, R., Szymkowiak, A. E., Seward, F. D., and Willingale, R., *ApJ* **335**, 215 (1988)
42. Shelton, R. L., Cox, D. P., Maciejewski, W., Smith, R. K., Plewa, T., Pawl, A., and Różyńska, M., *ApJ* **524**, 192 (1999)
43. Goss, W. M., *ApJS* **15**, 131 (1968)
44. Frail, D. A., Goss, W. M., and Slysh, V. I., *ApJ* **424**, L111 (1994)
45. Frail, D. A., Goss, W. M., Reynoso, E. M., Giacani, E. B., Green, A. J., and Otrupcek, R., *AJ* **111**, 1651 (1996)
46. Green, A. J., Frail, D. A., Goss, W. M., and Otrupcek, R., *AJ* **114**, 2058 (1997)
47. Koralesky, B., Frail, D. A., Goss, W. M., Claussen, M. J., and Green, A. J., *AJ* **116**, 1323 (1998)
48. Frail, D. A., and Mitchell, G. F., *ApJ* **508**, 690 (1998)
49. Reynoso, E. M., and Mangum, J. G., *ApJ* **545**, 874 (2000)
50. Reach, W. T., and Rho, J., *A&A* **315**, L277 (1996)
51. Reach, W. T., and Rho, J., *ApJ* **507**, L93 (1998)
52. Reach, W. T., and Rho, J., *ApJ* **544**, 843 (2000)
53. Reach, W. T., and Rho, J., *ApJ* **511**, 836 (1999)
54. Foster, P. N., and Boss, A. P., *ApJ* **468**, 784 (1996)
55. Vanhala, H. A. T., and Cameron, A. G. W., *ApJ* **508**, 291 (1999)
56. O'Dell, C. R., Wen, Z., and Hu, X., *ApJ* **410**, 696 (1993)
57. Chevalier, R. A., *ApJ* **538**, L151 (2000)